ANALYSIS OF CANTILEVER BEAM UNDER

ECCENTRIC DYNAMIC LOADING

by

Roy D. Stoyer

Submitted in Partial Fulfillment of the Requirements
for the Degree of
Master of Science in Engineering
in the
Mechanical Engineering
Program

Frank J. Tarantine March 15, 1978
Adviser Date

Leon Rand March 20, 1978
Dean of the Graduate School Date

YOUNGSTOWN STATE UNIVERSITY

March, 1978

ABSTRACT

ANALYSIS OF CANTILEVER BEAM UNDER
ECCENTRIC DYNAMIC LOADING

Roy D. Stoyer

Master of Science in Engineering

Youngstown State University, 1978

This thesis will present the basic equations necessary to predict the stresses produced in a cantilever beam when it is subjected to an eccentric dynamic load. These equations will then be discussed with respect to their advantages and disadvantages concerning the accuracy of their predictions and the simplicity of their applications. An explanation will next be given of an experimental model which was used to obtain data on this subject through the use of electrical resistance strain gages.

A comparison will then be made of the data obtained in this experiment with the data obtained through analytical treatment of the model. Following this is a concluding discussion on recommendations of methods for analyzing a cantilever beam subjected to eccentric dynamic loading.

TABLE OF CONTENTS

LIST OF SYMBOLS

SYMBOL	DEFINITION	VALUE	UNITS
b	Width of eccentric lever cross section	0.3125	in.
f_n	Natural frequency of system	20.45	cps
g	Acceleration due to gravity	386.09	in./sec^2
g_c	Gravatational constant	386.09	$\frac{\text{lbm - in.}}{\text{lbf - sec}^2}$
h	Drop height of weight		in.
h_R	Height of eccentric lever cross section	2.75	in.
k	Spring constant of weightless beam	360.13	$\frac{\text{lb}}{\text{in.}}$
ℓ	Length of weightless beam	39	in.
ℓ_g	Moment arm to strain gage location	28	in.
ℓ_1	Length of conduit	30	in.
ℓ_2	Length of eccentric lever	9	in.
m	Mass of falling weight	5	lbm
m_C	Mass of load cell	2.5	lbm
m_e	Equivalent mass for weightless beam (see Fig. 4.)		lbm
t	Time		sec
v_x	Velocity at any point X on weightless beam (see page 14)		$\frac{\text{in.}}{\text{sec}}$
v_ℓ	Velocity at end of weightless beam (see page 14)		$\frac{\text{in.}}{\text{sec}}$

LIST OF SYMBOLS

SYMBOL	DEFINITION	VALUE	UNITS
A_B	Cross sectional area of beam (conduit)	0.417	$in.^2$
A_L	Cross sectional area of eccentric lever	0.859	$in.^2$
A_P	Cross sectional area of pipe brace	0.80	$in.^2$
C	(See page 19)		lbf^2
$C_1 - C_6$	Constants of integration (see page 9 thru 14)		
D_1	Inside diameter of beam (conduit)	2.0625	in.
D_0	Outside diameter of beam (conduit)	2.1875	in.
E_B	Modulus of elasticity of beam (conduit)	30×10^6	$\frac{lb}{in.^2}$
E_L	Modulus of elasticity of eccentric lever	30×10^6	$\frac{lb}{in.^2}$
G	Modulus of rigidity of beam (conduit)	11.5×10^6	$\frac{lb}{in.^2}$
I_B	Moment of inertia of area of beam (conduit)	0.2357	$in.^4$
I_{cx}	Moment of inertia of area of 6 in. channel about X axis	15.1	$in.^4$
I_{cz}	Moment of inertia of area of 6 in. channel about Z axis	0.87	$in.^4$
I_L	Moment of inertia of area of eccentric lever	0.5416	$in.^4$
I_P	Moment of inertia of area of pipe brace	0.31	$in.^4$
J	Polar moment of inertia of area of beam (conduit)	0.4714	$in.^4$

LIST OF SYMBOLS

SYMBOL	DEFINITION	VALUE	UNITS
M	Bending moment		in.lb
P	Equivalent static load		lb
P_{yp}	Load required to cause yielding of beam (conduit)	208.59	lb
Q	(See page 6)		$\frac{in}{lb}$
T	Torque		in.lb
W	Weight of falling mass	5	lbf
α	(See Fig. 6.)	32.89	degrees
δ	Total deflection of beam and eccentric lever		in.
δ_x	Deflection at any point X of equivalent beam		in.
δ_1	Deflection at end of beam (conduit)		in.
δ_2	Deflection of eccentric lever due to bending		in.
$\delta_{2\ell}$	Deflection at end of equivalent beam		in.
ε_A	Measured experimental strain (see Tables 1 and 2)		$\frac{in.}{in.}$
ε_B	Measured experimental strain (see Tables 1 and 2)		$\frac{in.}{in.}$
ε_C	Measured experimental strain (see Tables 1 and 2)		$\frac{in.}{in.}$
θ	(See Fig. 6.)	16.09	degrees
γ	Poisson's Ratio	0.285	

LIST OF SYMBOLS

SYMBOL	DEFINITION	VALUE	UNITS
ρ	Density of steel	0.283	$\frac{lbm}{in.^3}$
σ	Bending stress		$\frac{lb}{in.^2}$
σ_{yp}	Bending stress at yield point for steel	30,000	$\frac{lb}{in.^2}$
σ_1	Principal bending stress (see Tables 1 and 2)		$\frac{lb}{in.^2}$
σ_2	Principal bending stress	0	$\frac{lb}{in.^2}$
σ_3	Principal bending stress (see Tables 1 and 2)		$\frac{lb}{in.^2}$
τ	Shear stress		$\frac{lb}{in.^2}$
ϕ	Angle of twist of beam (conduit) due to applied torque		radians
ω_n	Natural circular frequency of system	128.49	$\frac{radians}{sec}$
Σ	Summation of the mathematical terms that follow		

LIST OF FIGURES

LIST OF TABLES

CHAPTER I

Introduction

The subject being investigated in this thesis is the correlation between the results obtained by mathematical analysis of a cantilever beam subjected to an eccentric dynamic load and the results obtained by experimental analysis of the same beam subjected to the same loading. This type of beam and loading were selected due to the small amount of work that has been done in the field of combined stresses resulting from dynamic loading. There has been considerable work done concerning axial impact on a bar, transverse impact on a simply supported beam and torsional impact of a rod, but due to the complexity of mathematical analysis of combined stresses resulting from impact loading this latter field has yet to receive an exact mathematical treatment. There are several reasons for this lack of mathematical definition of the problem. One of these is that the complexity of the equations necessary to define the vibration of the beam and the accompanying propagation of stress waves in it make them impossible to solve unless some simplifying assumptions are made which in turn destroy the "exactness" of the solution. Hence, this thesis was undertaken to attempt to determine how some of these simplifying assumptions effect the solution to the problem. Some of the assumptions that will be considered are; the neglection of the mass of the beam; the neglection of energy loss in the form of heat; neglection of energy loss due to deformation of the impact surfaces; neglection of stress build-ups due to possible combining of elastic waves as they rebound back and forth through the beam and the assumption of plastic impact whereby the impacting bodies remain in contact rather than rebounding from each other as in an elastic impact. For the following investigations the metal will be considered to be homogeneous and of an isotropic polycrystalline structure and the stresses produced will be assumed to be in the elastic region of the metal.

CHAPTER II

THEORETICAL ANALYSIS OF BEAM

In this chapter the energy method will be used to develop the equations necessary to determine the stresses produced in a tubular cantilever beam when subjected to eccentric dynamic loading. The most basic approach is to neglect the mass of the beam and to assume that the loss in potential energy of the mass m in falling through some distance h is absorbed as strain energy by the beam. In this analysis it is assumed that there is an equivalent static load P that will produce the same deflection of the beam as the mass m falling through the height h. The work done by this equivalent static load is $P/2\delta$ where δ is the deflection of the beam at the point of load application. It is also assumed that the loads are such that buckling is not a factor. The beam configuration, loading and deflections caused by the falling weight mg are shown in Fig. 1.
From Fig. 1 comes the equation

$$\delta = \delta_1 + \ell_2 \sin \phi + \delta_2$$

where δ is the total deflection at point C. Using the assumption that for small angles of ϕ, $\phi = \sin \phi$ the above equation simplifies to

$$\delta = \delta_1 + \ell_2 \phi + \delta_2. \tag{1}$$

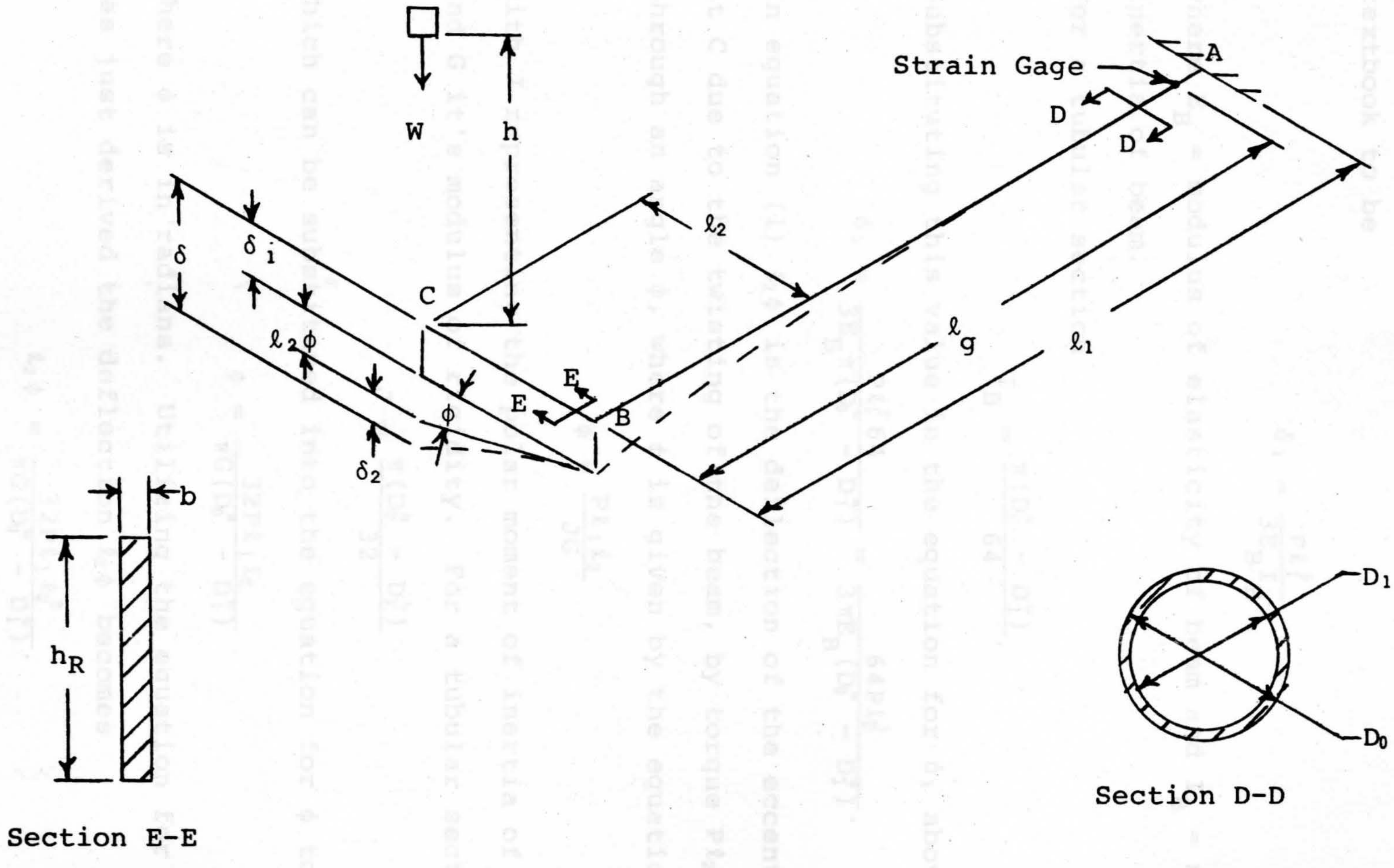

Fig. 1. Beam Configuration, Loading, Deflections and Associated Parameters.

δ_1 is the deflection of the beam at point B due to load P and can be found from any standard strength of materials textbook to be

$$\delta_1 = \frac{P\ell_1^3}{3E_B I_B}$$

where E_B = modulus of elasticity of beam and I_B = moment of inertia of beam.

For a tubular section

$$I_B = \frac{\pi(D_0^4 - D_i^4)}{64}.$$

Substituting this value in the equation for δ_1 above gives

$$\delta_1 = \frac{P\ell_1^3 64}{3E_B\pi(D_0^4 - D_i^4)} = \frac{64P\ell_1^3}{3\pi E_B(D_0^4 - D_i^4)}. \qquad (2)$$

In equation (1) $\ell_2\phi$ is the deflection of the eccentric lever at C due to the twisting of the beam, by torque $P\ell_2$, through an angle ϕ, where ϕ is given by the equation

$$\phi = \frac{P\ell_1\ell_2}{JG}$$

with J representing the polar moment of inertia of the beam and G it's modulus of rigidity. For a tubular section

$$J = \frac{\pi(D_0^4 - D_i^4)}{32}$$

which can be substituted into the equation for ϕ to produce

$$\phi = \frac{32P\ell_1\ell_2}{\pi G(D_0^4 - D_i^4)}$$

where ϕ is in radians. Utilizing the equation for ϕ that was just derived the deflection $\ell_2\phi$ becomes

$$\ell_2\phi = \frac{32P\ell_1\ell_2^2}{\pi G(D_0^4 - D_i^4)}. \qquad (3)$$

From Fig. 1, δ_2 is the deflection at C due to bending of the eccentric lever by load P and is given by

$$\delta_2 = \frac{P\ell_2^3}{3E_L I_L}$$

where E_L is the modulus of elasticity of the eccentric lever and I_L is it's moment of inertia. For the rectangular section of the eccentric lever, as shown in Fig. 1,

$$I_L = \frac{bh_R^3}{12}$$

and δ_2 becomes

$$\delta_2 = \frac{P\,\ell_2^3 12}{3E_L bh_R^3} = \frac{4P\ell_2^3}{E_L bh_R^3}. \tag{4}$$

Substituting equations (2), (3) and (4) into (1) produces the equation for the deflection δ.

$$\delta = \frac{64P\ell_1^3}{3\pi E_B(D_0^4 - D_i^4)} + \frac{32P\ell_1\ell_2^2}{\pi G(D_0^4 - D_i^4)} + \frac{4P\ell_2^3}{E_L bh_R^3}$$

This can be simplified to

$$\delta = PQ \tag{5}$$

where

$$Q = \left(\frac{32}{\pi(D_0^4 - D_i^4)}\left(\frac{2\ell_1^3}{3E_B} + \frac{\ell_1\ell_2^2}{G}\right) + \frac{4\ell_2^3}{E_L bh_R^3}\right).$$

Equating the loss in potential energy of the weight to the work done by the equivalent static load P produces the equation

$$W(h + \delta) = \frac{P}{2}\delta.$$

Substituting for δ from equation (5) produces the equation

$$W(h + PQ) = \frac{P}{2}(PQ)$$

which simplifies to

$$P^2 - 2WP - \frac{2Wh}{Q} = 0. \tag{6}$$

Solving equation (6) for P

$$P = \frac{2W + \left((-2W)^2 - 4\left(\frac{-2Wh}{Q}\right)\right)^{\frac{1}{2}}}{2}$$

$$P = W + \left(W^2 + \frac{2Wh}{Q}\right)^{\frac{1}{2}}. \tag{7}$$

The stresses produced in the beam by P can be found by the principal of superposition[1] whereby the separate effects of the moment $M = P\ell_g$ and the torque $T = P\ell_2$ are added. For the moment $M = P\ell_g$ the maximum bending stress occurs at

$$r = \frac{D_0}{2}$$

and is given by the equation

$$\sigma_{max} = \frac{MD_0/2}{I_B} = \frac{P\ell_g D_0}{2\left[\frac{\pi(D_0^4 - D_i^4)}{64}\right]} = \frac{32D_0 P\ell_g}{\pi(D_0^4 - D_i^4)}. \tag{8}$$

For the torque $T = P\ell_2$, the maximum shear stress occurs at

$$r = \frac{D_0}{2}$$

and is given by the equation

---

[1]John N. Cernica, Strength of Materials (Holt, Rinehart and Winston, Inc., 1966) p. 212.

$$\tau_{max} = \frac{T(D_0/2)}{J} = \frac{P\ell_2 D_0}{2\left[\frac{\pi(D_0^4 - D_i^4)}{32}\right]} = \frac{16 D_0 P \ell_2}{\pi(D_0^4 - D_i^4)}. \tag{9}$$

Now the principal stresses on an element at the surface of the beam can be found from the equation[2]

$$\left.\begin{matrix}\sigma_1\\ \sigma_3\end{matrix}\right\} = \frac{\sigma_{max}}{2} \pm \left[\left(\frac{\sigma_{max}}{2}\right)^2 + \left(\tau_{max}\right)^2\right]^{\frac{1}{2}}$$

which by substitution of equations (8) and (9) can be simplified to give the principal stresses

$$\sigma_1 = \frac{16 D_0 P}{\pi(D_0^4 - D_i^4)}\left[\ell_g + \left(\ell_g^2 + \ell_2^2\right)^{\frac{1}{2}}\right] \tag{10}$$

and

$$\sigma_3 = \frac{16 D_0 P}{\pi(D_0^4 - D_i^4)}\left[\ell_g - \left(\ell_g^2 + \ell_2^2\right)^{\frac{1}{2}}\right] \tag{11}$$

The derivation just completed did not consider the masses of the beam, the eccentric lever or the load cell (see Fig. 5). In neglecting these masses consideration was not given to the additional resistance to the motion of mass m that the inertia of these components produce. In order to include the mass of these components it is necessary to assume a mathematical relationship for their particle velocities during the period that they are in motion. A common assumption[2] is that the velocity of a point on the beam at any instant is proportional to the static deflection at that point. In order to derive an equation for the elastic line of the beam and eccentric lever, the deflection of the

---

[2]Frank A. D'Isa, Mechanics of Metals (Addison-Wesley Publishing Company, 1968) p. 19, p. 306.

eccentric lever due to twisting of the beam will be assumed to be small in relation to deflection by bending, and will be neglected. By doing this, the beam and eccentric lever can be treated as a straight cantilever beam and the equation for deflection of the beam and eccentric lever can be found by the integration method.[3] From the following equations

$$I_B = \frac{\pi(D_0^4 - D_I^4)}{64} = 0.2357 \text{ in}^4$$

$$I_L = \frac{bh_R^3}{12} = 0.5416 \text{ in}^4$$

the relationship that

$$I_L = 2.298\ I_B$$

can be established.

To begin the analysis for this condition by the integration method let M_1, θ_1 and δ_1 represent the equations for the beam for $0 \leq X \leq \ell_1$ and M_2, θ_2 and δ_2 represent the equations for the beam for $\ell_1 \leq X \leq (\ell_1 + \ell_2) = \ell$ and assume that $E_B = E_L = E$. Taking up as the positive direction for loads and clockwise as the positive direction for moments, integration produces the results in Fig. 2 and Fig. 3.

C_1 can be evaluated by applying the boundary condition, at $X = 0$, $M = -P\ell$, to the equation for M in Fig. 2.

$$-P\ell = P(0) + C_1$$

$$C_1 = -P\ell$$

---

[3]Cernica, Materials, pp. 224-231.

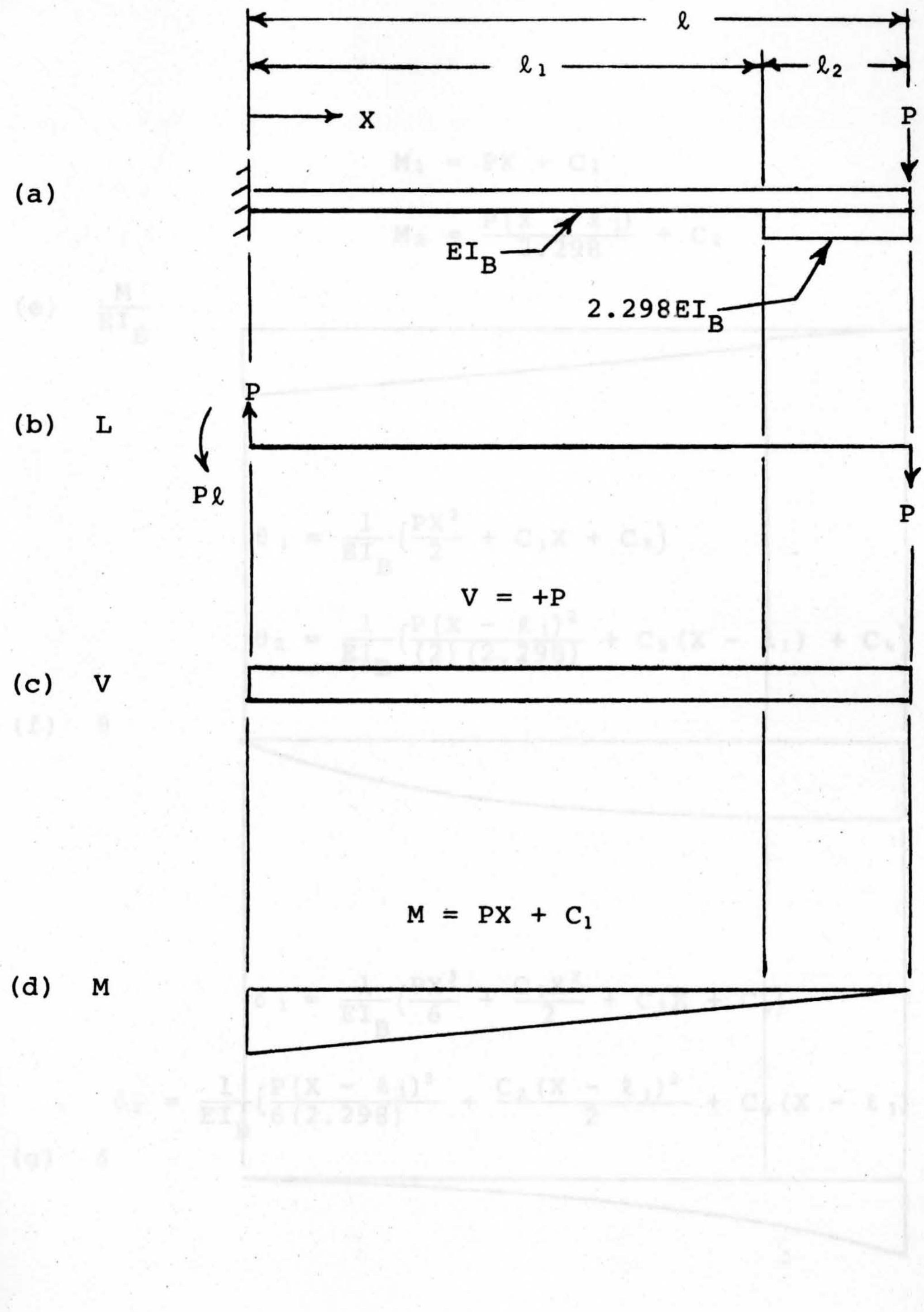

Fig. 2. Load, Shear and Moment Diagrams for Integration Method.

$$M_1 = PX + C_1$$

$$M_2 = \frac{P(X - \ell_1)}{2.298} + C_2$$

(e) $\frac{M}{EI_B}$

$$\theta_1 = \frac{1}{EI_B}\left(\frac{PX^2}{2} + C_1X + C_3\right)$$

$$\theta_2 = \frac{1}{EI_B}\left(\frac{P(X - \ell_1)^2}{(2)(2.298)} + C_2(X - \ell_1) + C_4\right)$$

(f) θ

$$\delta_1 = \frac{1}{EI_B}\left(\frac{PX^3}{6} + \frac{C_1X^2}{2} + C_3X + C_5\right)$$

$$\delta_2 = \frac{1}{EI_B}\left(\frac{P(X - \ell_1)^3}{6(2.298)} + \frac{C_2(X - \ell_1)^2}{2} + C_4(X - \ell_1) + C_6\right)$$

(g) δ

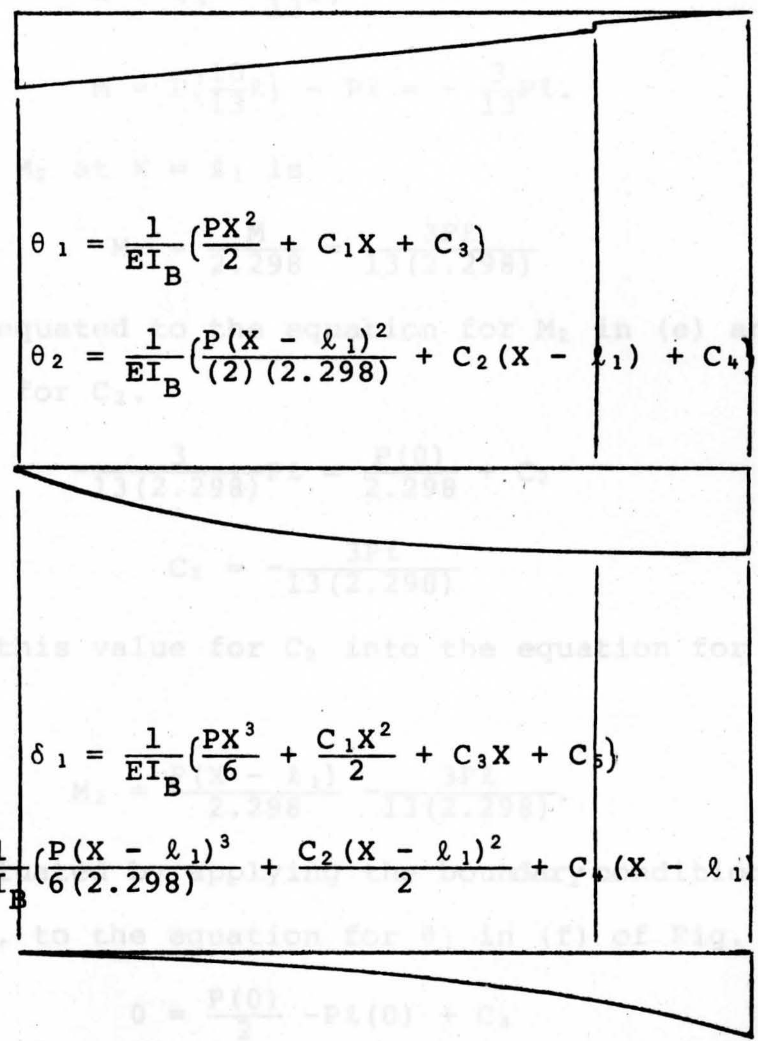

Fig. 3. M/EI_B, Slope and Deflection Diagrams for Integration Method.

Substituting this value for C_1 into the equation for M produces

$$M = PX - P\ell.$$

From (e) of Fig. 3, substituting C_1 from above,

$$M_1 = PX - P\ell.$$

C_2 can be evaluated by realizing that at

$$X = \ell_1 = \frac{10}{13}\ell,$$

$$M = P\left(\frac{10}{13}\ell\right) - P\ell = -\frac{3}{13}P\ell.$$

The value for M_2 at $X = \ell_1$ is

$$M_2 = \frac{M}{2.298} = \frac{3P\ell}{13(2.298)}$$

which can be equated to the equation for M_2 in (e) and the result solved for C_2.

$$-\frac{3}{13(2.298)}P\ell = \frac{P(0)}{2.298} + C_2$$

$$C_2 = -\frac{3P\ell}{13(2.298)}$$

Substituting this value for C_2 into the equation for M_2 produces

$$M_2 = \frac{P(X - \ell_1)}{2.298} - \frac{3P\ell}{13(2.298)}.$$

C_3 can be evaluated by applying the boundary condition, at $X = 0$, $\theta_1 = 0$, to the equation for θ_1 in (f) of Fig. 3.

$$0 = \frac{P(0)}{2} - P\ell(0) + C_3$$

$$C_3 = 0$$

Substituting the values for C_1 and C_3 into the equation for θ_1 produces

$$\theta_1 = \frac{P}{EI_B}\left(\frac{X^2}{2} - \ell X\right).$$

C_4 can be evaluated by using the condition that at $X = \ell_1$, $\theta_1 = \theta_2$. Applying this principle produces

$$\theta_1 = \frac{P}{EI_B}\left(\frac{\left(\frac{10}{13}\ell\right)^2}{2} - \ell\left(\frac{10}{13}\ell\right)\right)$$

$$\theta_1 = -\frac{80P\ell^2}{169EI_B}.$$

Equating θ_1 and θ_2 at $X = \ell_1$ and solving for C_4 produces

$$-\frac{80P\ell^2}{169EI_B} = 0 + 0 + C_4\,\frac{1}{EI_B}$$

which yields

$$C_4 = -\frac{80}{169}P\ell^2.$$

Substituting the values for C_2 and C_4 into the equation for θ_2 produces

$$\theta_2 = \frac{P}{EI_B}\left(\frac{(X - \ell_1)^2}{(2)(2.298)} - \frac{3\ell(X - \ell_1)}{13(2.298)} - \frac{80}{169}\ell^2\right).$$

C_5 can be found from the equation for δ_1 in Fig. 3 by using the boundary condition, at $X = 0$, $\delta_1 = 0$.

$$0 = 0 + 0 + 0 + C_5$$

$$C_5 = 0$$

Substituting the values for C_1, C_3 and C_5 into the equation for δ_1 produces

$$\delta_1 = \frac{P}{EI_B}\left(\frac{X^3}{6} - \frac{\ell X^2}{2}\right) \qquad (12)$$

C_6 can be evaluated by using the condition that at $X = \ell_1$, $\delta_1 = \delta_2$. Applying this principle produces

$$\delta_1 = \frac{P}{EI_B}\left(\frac{\left(\frac{10}{13}\ell\right)^3}{6} - \frac{\ell\left(\frac{10}{13}\ell\right)^2}{2}\right)$$

which can be simplified and equated to δ_2 at $X = \ell_1$ to find C_6.

$$C_6 = -\frac{1450P\ell^3}{6591EI_B}$$

Substituting C_2, C_4 and C_6 into the equation for δ_2 produces

$$\delta_2 = \frac{P}{EI_B}\left[\frac{(X - \ell_1)^3}{13.788} - \frac{3\ell(X - \ell_1)^2}{59.748} - \frac{80\ell^2(X - \ell_1)}{169} - \frac{1450}{6591}\ell^3\right]. \tag{13}$$

Evaluating δ_2 at $X = \ell$ produces

$$\delta_{2_\ell} = -0.331\frac{P\ell^3}{EI_B} \tag{14}$$

which is the deflection at the end of the beam.

Assuming the velocity relationship

$$\frac{v_x}{\delta_x} = \frac{v_\ell}{\delta_\ell} = \frac{v_\ell}{\delta_{2_\ell}}$$

$$v_x = v_\ell \frac{\delta_x}{\delta_{2_\ell}}$$

where δ_x and v_x represent the deflection and velocity, respectively, at any point x on the beam and v_ℓ represents the velocity at the end of the beam. Equations (12), (13) and (14) can be used to establish the relationships:

$$-\frac{\delta_1}{\delta_{2_\ell}} = \frac{\frac{P}{EI_B}\left(\frac{X^3}{6} - \frac{\ell X^2}{2}\right)}{\frac{0.331P\ell^3}{EI_B}} = \frac{0.504(X^3 - 3\ell X^2)}{\ell^3}$$

and

$$-\frac{\delta_2}{\delta_{2\ell}} = \frac{0.219(X - \ell_1)^3}{\ell^3} - \frac{0.152(X - \ell_1)^2}{\ell^2} - \frac{1.430(X - \ell_1)}{\ell} - 0.665$$

from which the expression for the total kinetic energy of the beam, lever and load cell can be written

$$(KE)_{BLC} = \int_0^{\ell_1} \tfrac{1}{2}(v_\ell)^2 \left(\frac{0.504(X^3 - 3\ell X^2)}{\ell^3}\right)^2 \rho A_B \, dx$$

$$+ \int_{\ell_1}^{\ell} \tfrac{1}{2}(v_\ell)^2 \left\{\frac{0.219(X - \ell_1)^3}{\ell^3} - \frac{0.152(X - \ell_1)^2}{\ell^2}\right.$$

$$\left. - \frac{1.430(X - \ell_1)}{\ell} - 0.665\right\}^2 \rho A_L \, dx + \tfrac{1}{2}m_c(v_\ell)^2.$$

In the above equation ρ = density of the beam = density of the lever, A_B = cross sectional area of beam and A_ℓ = cross sectional area of lever.

Integrating the first integral of the equation for total kinetic energy,

$$\frac{(0.504)^2 \rho A_B}{2\ell^6} v_\ell^2 \left(\int_0^{\ell_1} X^6 dx - 6\ell \int_0^{\ell_1} X^5 dx + 9\ell^2 \int_0^{\ell_1} X^4 dx\right)$$

$$= \frac{(0.504)^2 \rho A_B}{2\ell^6} v_\ell^2 \left(\left(\frac{X^7}{7}\right|_0^{\ell_1} - 6\ell\left(\frac{X^6}{6}\right|_0^{\ell_1} + 9\ell^2\left(\frac{X^5}{5}\right|_0^{\ell_1}\right)$$

and by substituting $\ell_1 = 10/13\ell$ in the expression above, it simplifies to

$$\tfrac{1}{2}(0.0763\rho A_B \ell)\, v_\ell^2.$$

The second integral of the equation for total kinetic energy simplifies into the sum of the following integrals:

$$\frac{(0.219)^2}{\ell^6}\int_{\ell_1}^{\ell} (X - \ell_1)^6\, dx = \frac{(0.219)^2}{\ell^6}\left(\frac{(X - \ell_1)^7}{7}\right|_{\ell_1}^{\ell}$$

$$= 2.39 \times 10^{-7}\ell$$

$$\frac{2(0.219)(0.152)}{\ell^5}\int_{\ell_1}^{\ell} (X - \ell_1)^5\, dx = \frac{2(0.219)(0.152)}{\ell^5}\left(\frac{(X - \ell_1)^6}{6}\right|_{\ell_1}^{\ell}$$

$$= 1.68 \times 10^{-6}\ell$$

$$\frac{2(0.219)(1.430)}{\ell^4}\int_{\ell_1}^{\ell} (X - \ell_1)^4\, dx = \frac{2(0.219)(1.430)}{\ell^4}\left(\frac{(X - \ell_1)^5}{5}\right|_{\ell_1}^{\ell}$$

$$= 8.20 \times 10^{-5}\ell$$

$$\frac{2(0.219)(0.665)}{\ell^3}\int_{\ell_1}^{\ell} (X - \ell_1)^3\, dx = \frac{2(0.219)(0.665)}{\ell^3}\left(\frac{(X - \ell_1)^4}{4}\right|_{\ell_1}^{\ell}$$

$$= 2.07 \times 10^{-4}\ell$$

$$\frac{(0.152)^2}{\ell^4}\int_{\ell_1}^{\ell} (X - \ell_1)^4\, dx = \frac{(0.152)^2}{\ell^4}\left(\frac{(X - \ell_1)^5}{5}\right|_{\ell_1}^{\ell}$$

$$= 3.02 \times 10^{-6}\ell$$

$$\frac{2(0.152)(1.430)}{\ell^3}\int_{\ell_1}^{\ell} (X - \ell_1)^3\, dx = \frac{2(0.152)(1.430)}{\ell^3}\left(\frac{(X - \ell_1)^4}{4}\right|_{\ell_1}^{\ell}$$

$$= 3.08 \times 10^{-4}\ell$$

$$\frac{2(0.152)(0.665)}{\ell^2}\int_{\ell_1}^{\ell} (X - \ell_1)^2\, dx = \frac{2(0.152)(0.665)}{\ell^2}\left(\frac{(X - \ell_1)^3}{3}\right|_{\ell_1}^{\ell}$$

$$= 8.28 \times 10^{-4}\ell$$

$$\frac{(1.430)^2}{\ell^2}\int_{\ell_1}^{\ell} (X - \ell_1)^2\, dx = \frac{(1.430)^2}{\ell^2}\ \frac{(X - \ell_1)^3}{3}\Big|_{\ell_1}^{\ell}$$

$$= 8.38 \times 10^{-3}\ell$$

$$\frac{2(1.430)(0.665)}{\ell}\int_{\ell_1}^{\ell} (X - \ell_1)\, dx = \frac{2(1.430)(0.665)}{\ell}\left(\frac{(X - \ell_1)^2}{2}\right|_{\ell_1}^{\ell}$$

$$= 5.06 \times 10^{-2}\ell$$

Combining the above results produces the equation

$$\tfrac{1}{2}(v_\ell)^2 \rho A_L \int_{\ell_1}^{\ell} \left(\frac{0.219(X - \ell_1)^3}{\ell^3} - \frac{0.152(X - \ell_1)^2}{\ell^2} - \frac{1.430(X - \ell_1)}{\ell} - 0.665\right)^2 dx$$

$$= \tfrac{1}{2}\left(0.0599\rho A_L \ell\right) v_\ell^2 .$$

Then the expression for the total kinetic energy of the beam, lever and load cell becomes

$$(KE)_{BLC} = \tfrac{1}{2}(0.0763\rho A_B \ell) v_\ell^2 + \tfrac{1}{2}(0.0599\rho A_L \ell)(v_\ell)^2 + \tfrac{1}{2} m_C v_\ell^2$$

which simplifies to

$$(KE)_{BLC} = \tfrac{1}{2}\left[\rho\ell(0.0763A_B + 0.0599A_L) + m_C\right] v_\ell^2 . \qquad (15)$$

Equation (15) shows that the original system as shown in Fig. 5 can be replaced by the equivalent weightless beam and concentrated mass system shown in Fig. 4.

Applying the principal of conservation of linear momentum to the falling mass and equivalent mass system for an assumed perfectly plastic impact, where $\sqrt{2gh}$ equals the velocity of the falling mass at the instant of impact, produces

$$m\sqrt{2gh} = \left(\rho\ell(0.0763A_B + 0.0599A_L + m_C + m\right) v_\ell$$

where

$$v_\ell = \frac{m\sqrt{2gh}}{\left(\rho\ell(0.0763A_B + 0.0599A_L) + m_C + m\right)}$$

which is the velocity of the falling mass and equivalent mass immediately after impact. Then the total kinetic

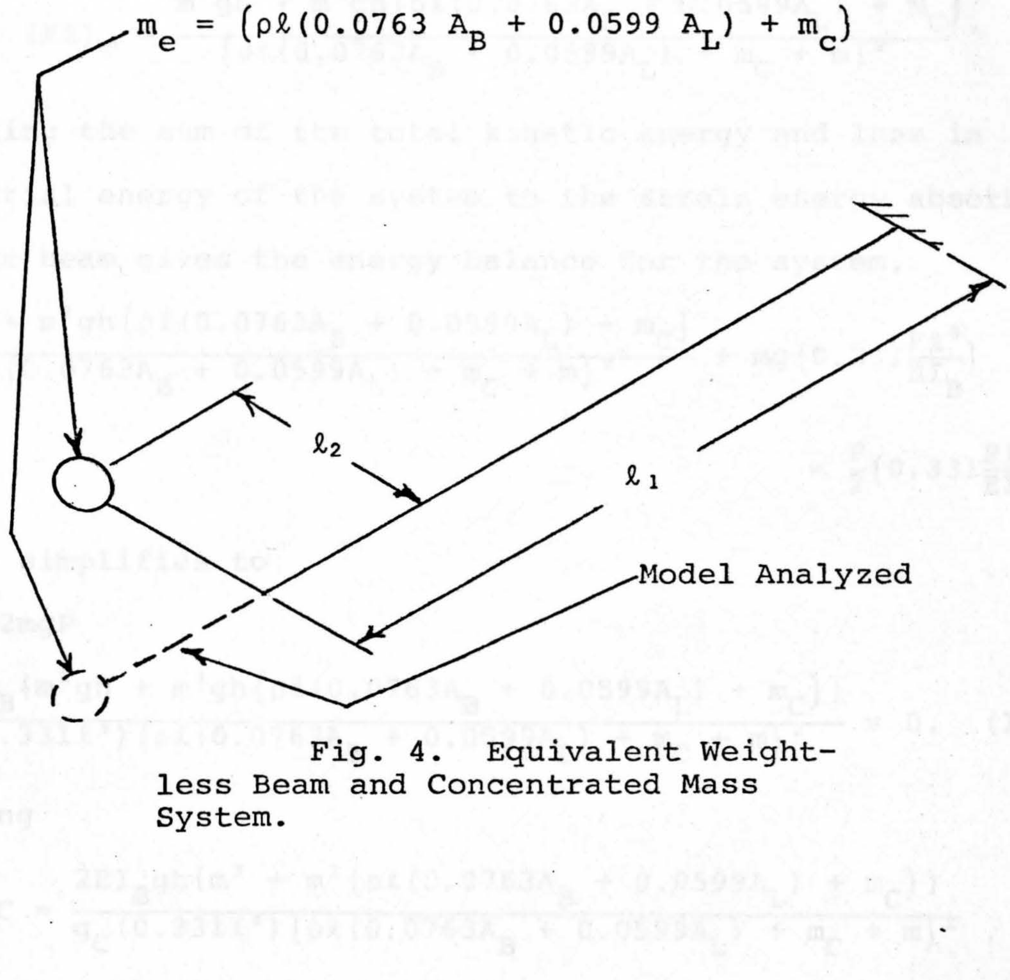

Fig. 4. Equivalent Weightless Beam and Concentrated Mass System.

energy of the masses immediately after impact is given by the equation

$$(KE)_T = \tfrac{1}{2}m(v_\ell)^2 + \tfrac{1}{2}m_e(v_\ell)^2$$

which can be simplified to

$$(KE)_T = \frac{m^3gh + m^2gh\left(\rho\ell(0.0763A_B + 0.0599A_L) + m_C\right)}{\left(\rho\ell(0.0763A_B + 0.0599A_L) + m_C + m\right)^2}.$$

Equating the sum of the total kinetic energy and loss in potential energy of the system to the strain energy absorbed by the beam gives the energy balance for the system,

$$\frac{m^3gh + m^2gh\left(\rho\ell(0.0763A_B + 0.0599A_L) + m_C\right)}{\left(\rho\ell(0.0763A_B + 0.0599A_L) + m_C + m\right)^2} + mg\left(0.331\frac{P\ell^3}{EI_B}\right)$$

$$= \frac{P}{2}\left(0.331\frac{P\ell^3}{EI_B}\right)$$

which simplifies to

$$P^2 - 2mgP - \frac{2EI_B\{m^3gh + m^2gh\left(\rho\ell(0.0763A_B + 0.0599A_L) + m_C\right)\}}{(0.331\ell^3)\left(\rho\ell(0.0763A_B + 0.0599A_L) + m_C + m\right)^2} = 0. \quad (16)$$

Letting

$$C = \frac{2EI_Bgh\{m^3 + m^2\left(\rho\ell(0.0763A_B + 0.0599A_L) + m_C\right)\}}{g_C(0.331\ell^3)\left(\rho\ell(0.0763A_B + 0.0599A_L) + m_C + m\right)^2}$$

and

$$A_B = \pi\left\{\left(\frac{D_0}{2}\right)^2 - \left(\frac{D_1}{2}\right)^2\right\}$$

$$A_L = bh_R$$

$$g_C = \text{gravitational constant}$$

equation (16) becomes

$$P^2 - 2mgP - C = 0. \quad (17)$$

Solving (17) for P, the equivalent static load,

$$P = \frac{2mg \pm \sqrt{(2mg)^2 + 4C}}{2}$$

which simplifies to

$$P = \left(\frac{mg}{g_C}\right) + \left[\left(\frac{mg}{g_C}\right)^2 + C\right]^{\frac{1}{2}}. \qquad (18)$$

P can then be substituted into equations (10) and (11) to obtain the principal stresses σ_1 and σ_3 for the beam.

Through the application of Newton's second law of motion to the sum of the masses, the time required to develop P can be found, along with the natural frequency of vibration of the undamped system. From (14) the spring constant k of the bar is found to be

$$k = -\frac{EI_B}{0.331\ell^3}.$$

Applying Newton's second law to the system produces the equations

$$\left(\rho\ell(0.0763A_B + 0.0599A_L) + m_C + m\right)\frac{d^2\delta_{2\ell}}{dt^2} = -\frac{EI_B}{0.331\ell^3}\delta_{2\ell}$$

$$\frac{d^2\delta_{2\ell}}{dt^2} + \frac{EI_B g_C}{0.331\ell^3\left(\rho\ell(0.0763A_B + 0.0599A_L) + m_C + m\right)}\delta_{2\ell} = 0$$

which can be simplified to

$$\frac{d^2\delta_{2\ell}}{dt^2} + \omega_n^2\delta_{2\ell} = 0 \qquad (19)$$

by letting

$$\omega_n^2 = \frac{EI_B g_C}{0.331\ell^3\left(\rho\ell(0.0763A_B + 0.0599A_L) + m_C + m\right)}. \qquad (20)$$

The solution of equation (19) can be found to be[4]

$$\delta_{2_\ell} = C_1 \cos\omega_n t + C_2 \sin\omega_n t.$$

Using the initial and boundary conditions, $d\delta_{2_\ell}/dt = v_\ell$ at $t = 0$ and $\delta_{2_\ell} = 0$ at $t = 0$, C_1 can be found to equal zero and $C_2 = v_\ell/\omega_n$. Then the equation for δ_{2_ℓ} becomes

$$\delta_{2_\ell} = \frac{v_\ell}{\omega_n}\sin\omega_n t$$

which is the equation of motion for the system. Differentiating δ_{2_ℓ} produces the equation

$$\frac{d\delta_{2_\ell}}{dt} = v_\ell \cos\omega_n t.$$

Now if $d\delta_{2_\ell}/dt$ is to equal zero ω_n must equal $\pi/2$ or

$$t = \frac{\pi}{2\omega_n} \tag{21}$$

which is the time required to develop the force P and is also one fourth of the period of vibration of the system. The constant ω_n is found from a study of vibrations[5] to be the natural circular frequency of vibration of the system and from it the natural frequency of vibration is

$$f_n = \frac{\omega_n}{2\pi}. \tag{22}$$

---

[4]Robert F. Streidel, Jr., <u>An Introduction to Mechanical Vibrations</u> (John Wiley & Sons, Inc., 1971) p. 39.

[5]Streidel, <u>Vibrations</u>, p. 41.

From equations (21) and (20)

$$t = \frac{\pi\{0.331\ell^3(\rho\ell(0.0763A_B + 0.0599A_L) + m_C + m)\}^{\frac{1}{2}}}{2(g_C E I_B)^{\frac{1}{2}}} \quad (23)$$

and from equations (22) and (20)

$$f_n = \frac{(g_C E I_B)^{\frac{1}{2}}}{2\pi\{0.331\ell^3(\rho\ell(0.0763A_B + 0.0599A_L) + m_C + m)\}^{\frac{1}{2}}}. \quad (24)$$

CHAPTER III

TEST APPARATUS AND EXPERIMENTAL PROCEDURE

Before the experimental process could proceed it was first necessary to determine the load that could safely be applied to the test apparatus. The allowable load on the test apparatus is governed by the size of the electrical conduit and can be found through the use of equations (10) and (11) and the octahedral shear stress theory. Assuming the yield strengths of the metal to be equal in tension and compression and applying the octahedral shear stress theory produces the relationship[6]

$$(\sigma_1 - \sigma_2)^2 + (\sigma_2 - \sigma_3)^2 + (\sigma_3 - \sigma_1)^2 = 2\sigma_{yp}^2. \qquad (25)$$

Let P_{yp} equal the maximum allowable load that the conduit will take without yielding. Adapting equations (10) and (11) to the situation (10) becomes

$$\sigma_1 = \frac{16D_0P_{yp}}{\pi(D_0^4 - D_i^4)}\left(\ell_1 + \sqrt{\ell_1^2 + \ell_2^2}\right)$$

and equation (11) becomes

$$\sigma_3 = \frac{16D_0P_{yp}}{\pi(D_0^4 - D_i^4)}\left(\ell_1 - \sqrt{\ell_1^2 + \ell_2^2}\right).$$

Substituting in equation (25) with $\sigma_2 = 0$ produces

---

[6]D'Isa, <u>Metals</u>, p. 153.

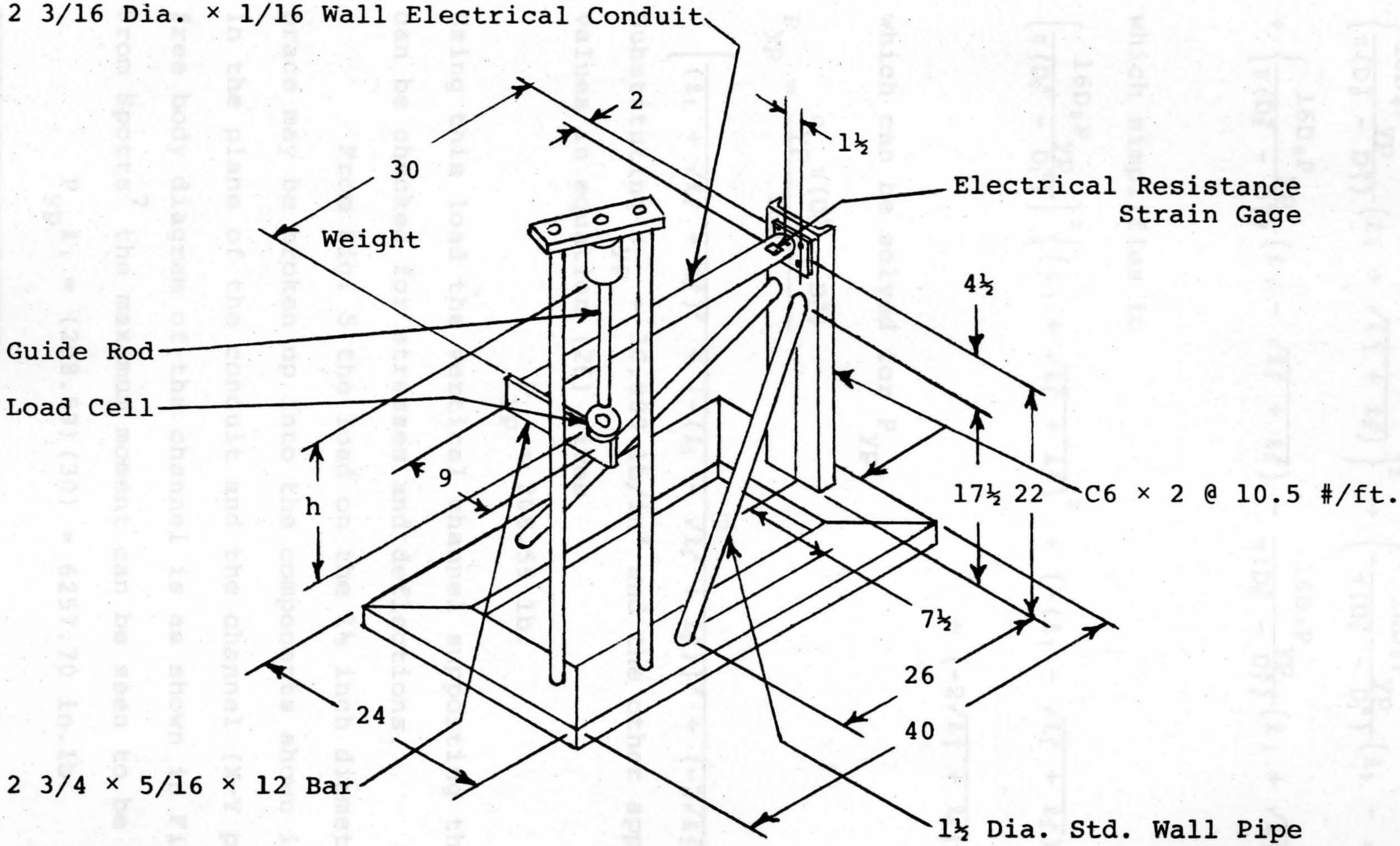

Fig. 5. Test Apparatus.

$$\left\{\frac{16D_0P_{yp}}{\pi(D_0^4 - D_1^4)}\left(\ell_1 + \sqrt{\ell_1^2 + \ell_2^2}\right)\right\}^2 + \left\{-\frac{16D_0P_{yp}}{\pi(D_0^4 - D_1^4)}\left(\ell_1 - \sqrt{\ell_1^2 + \ell_2^2}\right)\right\}^2$$

$$+ \left\{\frac{16D_0P_{yp}}{\pi(D_0^4 - D_1^4)}\left(\ell_1 - \sqrt{\ell_1^2 + \ell_2^2}\right) - \frac{16D_0P_{yp}}{\pi(D_0^4 - D_1^4)}\left(\ell_1 + \sqrt{\ell_1^2 + \ell_2^2}\right)\right\}^2 = 2\sigma_{yp}^2$$

which simplifies to

$$\left(\frac{16D_0P_{yp}}{\pi(D_0^4 - D_1^4)}\right)^2\left\{\left(\ell_1 + \sqrt{\ell_1^2 + \ell_2^2}\right)^2 + \left(-(\ell_1 - \sqrt{\ell_1^2 + \ell_2^2})\right)^2 + \left(-2\sqrt{\ell_1^2 + \ell_2^2}\right)^2\right\} = 2\sigma_{yp}^2$$

which can be solved for P_{yp}.

$$P_{yp} = \frac{\sigma_{yp}\pi(D_0^4 - D_1^4)}{16D_0}\left[\frac{2}{(\ell_1 + \sqrt{\ell_1^2 + \ell_2^2})^2 + \left(-(\ell_1 - \sqrt{\ell_1^2 + \ell_2^2})\right)^2 + (-2\sqrt{\ell_1^2 + \ell_2^2})^2}\right]^{1/2} \tag{26}$$

Substituting $\sigma_{yp} = 30{,}000$ lb/in^2 and the other appropriate values in equation (26) gives

$$P_{yp} = 208.59 \text{ lb.}$$

Using this load the vertical channel supporting the conduit can be checked for stresses and deflections.

From Fig. 5 the load on the 1½ inch diameter pipe brace may be broken up into the components shown in Fig. 6. In the plane of the conduit and the channel (X-Y plane) the free body diagram of the channel is as shown in Fig. 7. From Spotts[7] the maximum moment can be seen to be

$$P_{yp}\ell_1 = (208.59)(30) = 6257.70 \text{ in.lb}$$

---

[7] M. F. Spotts, Design of Machine Elements (Prentice-Hall, Inc., Englewood Cliffs, N. J., 1971), p.21.

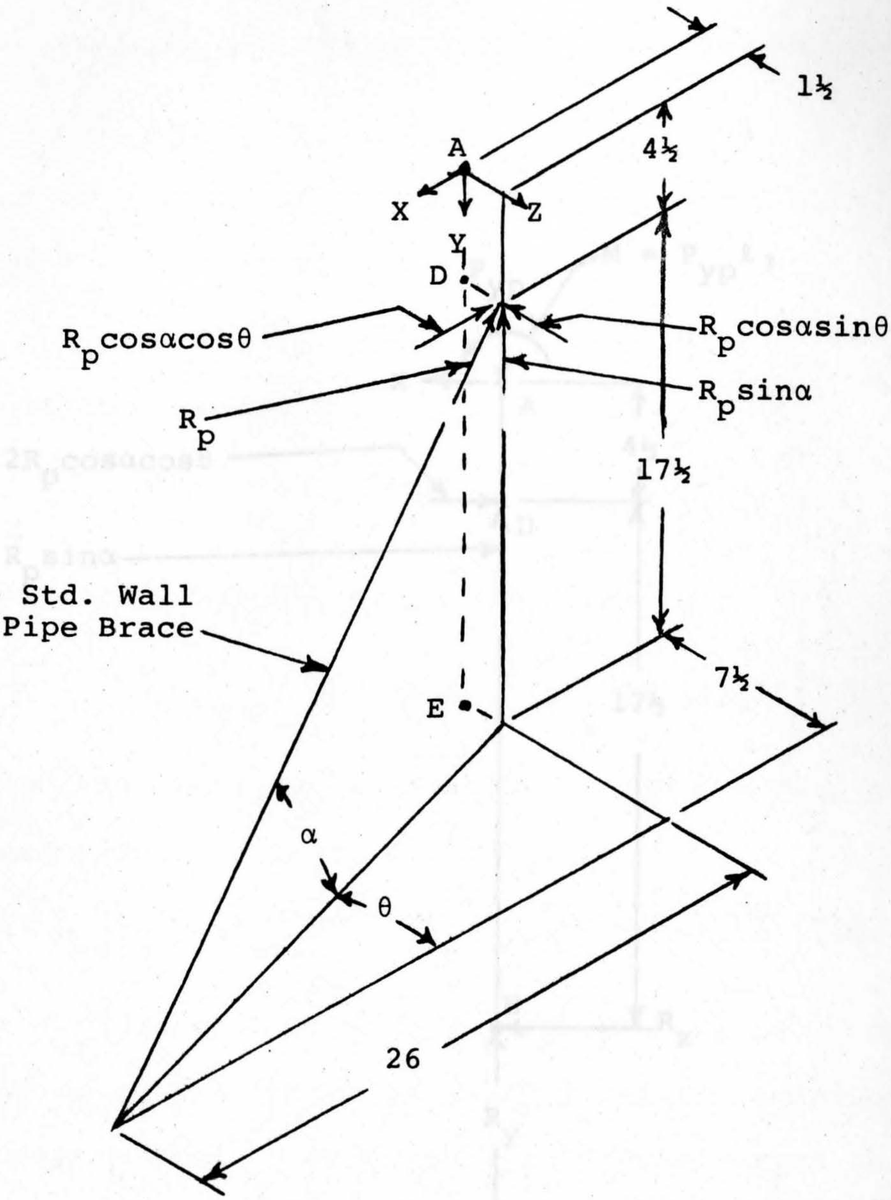

Fig. 6. Force Components for Pipe Brace.

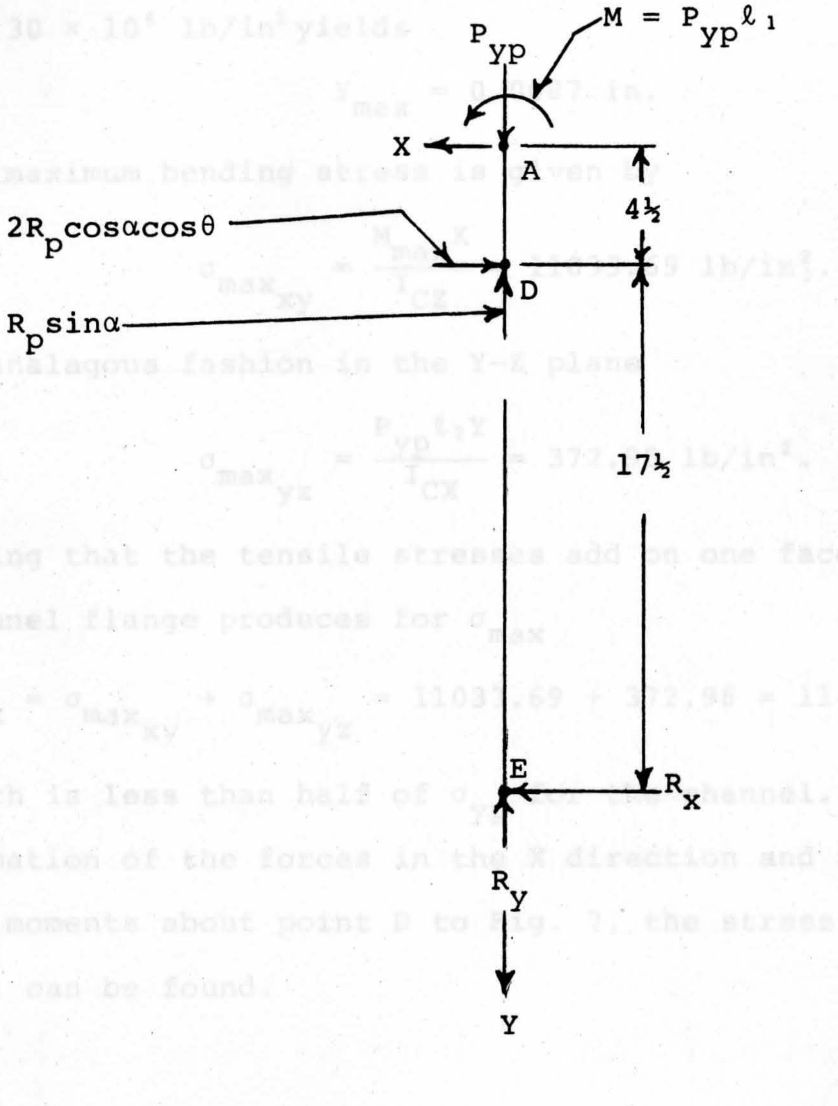

Fig. 7. Free Body Diagram of Vertical Channel.

and the maximum deflection, which occurs at A, is given by the equation

$$Y_{max} = \frac{P_{yp}\ell_1(4.5)}{6EI_{CZ}}\left(2(17.5) + 3(4.5)\right)$$

which upon substitution of the values $I_{CZ} = 0.87\ in^4$ = the moment of inertia of the channel about the Z axis and $E = 30 \times 10^6\ lb/in^2$ yields

$$Y_{max} = 0.0087\ in.$$

The maximum bending stress is given by

$$\sigma_{max_{xy}} = \frac{M_{max}X}{I_{CZ}} = 11033.69\ lb/in^2.$$

In analagous fashion in the Y-Z plane

$$\sigma_{max_{yz}} = \frac{P_{yp}\ell_2 Y}{I_{CX}} = 372.98\ lb/in^2.$$

Noting that the tensile stresses add on one face of the channel flange produces for σ_{max}

$$\sigma_{max} = \sigma_{max_{xy}} + \sigma_{max_{yz}} = 11033.69 + 372.98 = 11406.67\ lb/in^2$$

which is less than half of σ_{yp} for the channel. By applying summation of the forces in the X direction and summation of the moments about point D to Fig. 7, the stress in the pipe (σ_p) can be found.

$$\Sigma F_x = 0$$

$$2R_p \cos\alpha\cos\theta = R_x$$

$$\Sigma M_D = 0$$

$$P_{yp}\ell_1 = R_x(17.5)$$

$$R_x = \frac{P_{yp}\ell_1}{17.5} = \frac{6257.70}{17.5} = 357.58 \text{ lb}$$

$$R_p = \frac{R_x}{2\cos\alpha\cos\theta} = \frac{357.58}{2(\cos 32.89 \cos 16.09)} = 221.60 \text{ lb}$$

$$\sigma_p = \frac{R_p}{A_p} = \frac{221.60}{0.80} = 277.19 \text{ lb/in}^2 << \sigma_{yp}$$

The critical load (P_{CR}) required to cause buckling of the pipe brace can be found from Euler's (pinned end) column equation.

$$P_{CR} = \frac{\pi^2 EI_P}{L^2}$$

$$I_p = \frac{\pi\left[(1.90)^4 - (1.61)^4\right]}{64} = 0.31 \text{ in}^4$$

$$P_{CR} = \frac{\pi^2(30 \times 10^6)(0.31)}{\left[(26)^2 + (7.5)^2 + (17.5)^2\right]} = 88384 \text{ lb} >>> R_p$$

Since the shear and compression loads in the vertical channel and in the channel base are small they require no further consideration. From the above analysis it can be concluded that the strength of the test frame is more than adequate to sustain a load sufficient to cause yielding of the conduit. It should also be noted that deflection of the vertical channel at A was found to be small. In view of this, the strain energy absorbed by the frame will be considered to be small in relation to that absorbed by the conduit and will be neglected.

The experiment was begun by calibrating the load cell mounted on the eccentric lever. The equipment selected for use in this experiment, a Century 447 oscillograph using Ellis BA-4 amplifiers, was connected to the four active arm strain gage bridge in the load cell and then the bridge was balanced. A 20 pound weight was then placed on the load cell and a strip chart ran to record the deflection of the light beam on the chart corresponding to this weight. This process was repeated as the load was increased in 20 pound increments until a load of 160 pounds was reached. At this point the recording equipment was connected to the electrical resistance strain gages on the cantilever beam (see Fig. 8) and on the piece of conduit which was used to mount a "dummy" gage for temperature compensation. The strain gages employed were 350 ohm rectangular rosettes manufactured by Micro-Measurements, Romulus, Michigan (gage no. CEA-06-12SUR-350). The strain gages were connected in such a manner as to form three wheatstone bridges, each with one active arm on the cantilever beam and one "dummy" arm on the piece of conduit lying next to the test apparatus. The orientation of the strain gages on the pieces of conduit were as shown in Fig. 8.

After these bridges were balanced, the weight was dropped on the load cell from heights of ½ inch, 1 inch,

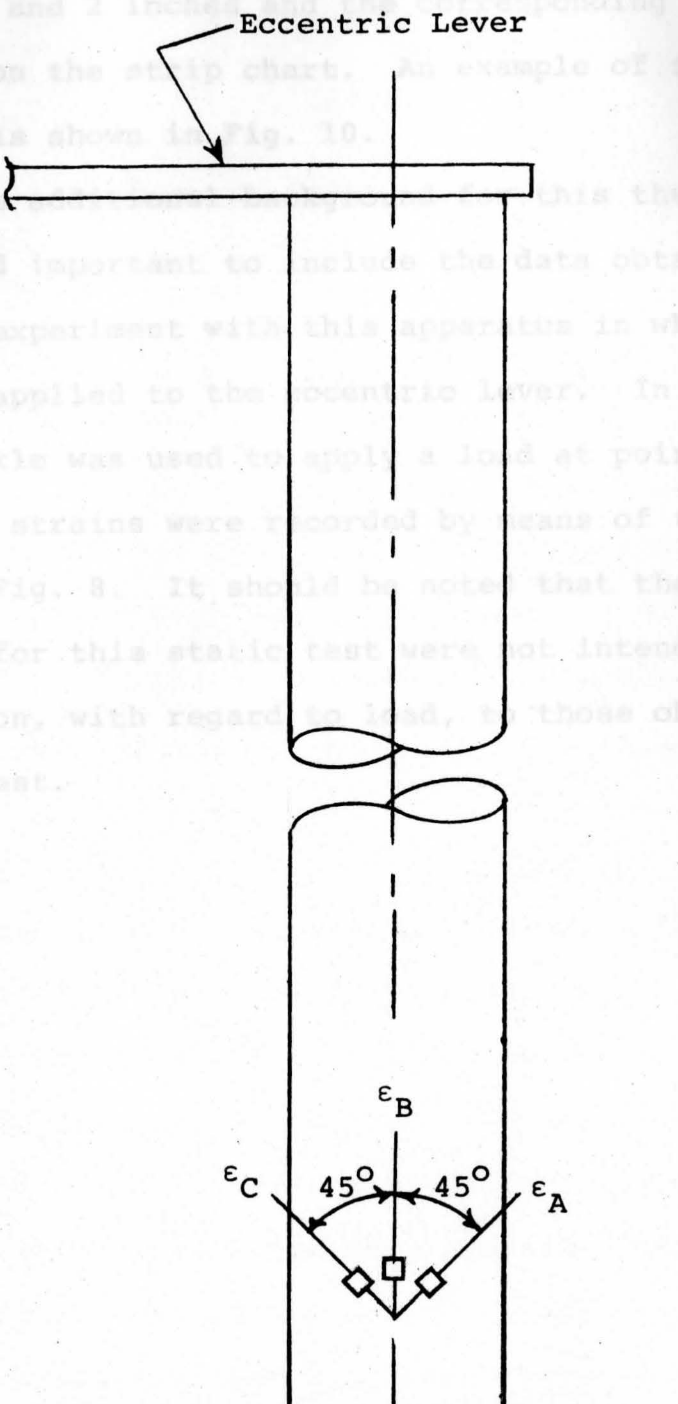

Fig. 8. Orientation of
Strain Gages on Cantilever Beam

1½ inches and 2 inches and the corresponding strains recorded on the strip chart. An example of the strains recorded is shown in Fig. 10.

As additional background for this thesis, it was considered important to include the data obtained in a previous experiment with this apparatus in which a static load was applied to the eccentric lever. In this experiment a turnbuckle was used to apply a load at point C in Fig. 1 while the strains were recorded by means of the strain gages shown in Fig. 8. It should be noted that the strains recorded for this static test were not intended to show any correlation, with regard to load, to those obtained in the dynamic test.

CHAPTER IV

SUMMARY OF RESULTS AND CONCLUSIONS

The data obtained from the mathematical analysis of the test apparatus along with that obtained by experimental means is listed in Tables 1 and 2. Table 1 lists the data for dynamic loading of the beam by means of a falling weight while Table 2 lists that obtained when a static load was applied to the eccentric lever, at $\ell_2 = 9$ in, by means of a turnbuckle. The principal stresses resulting from the four different methods of analysis are shown in graph form in Fig. 9.

From Fig. 9 it can be seen that the principal stresses obtained by mathematical means, when the inertia of the mass of the beam, lever and load cell were considered came the closest to those obtained by actual measurement of the dynamic strains in the beam. It should be noted from Fig. 9, that as the analysis moved from the static test to the final experimental dynamic analysis, consideration of the inertia effects of the masses caused the graph of the derived principal stresses to move closer to the graph of the experimental principal stresses. As inertia was considered the value of σ_1 corresponding to a particular drop height h decreased and moved toward the experimental value of σ_1. In the same fashion σ_3 can be seen to become less negative as inertia was considered and move toward the

TABLE 1

RESULTS OF DYNAMIC TESTS AND ANALYSIS

Weight Drop Height (in)	Experimental Strains (Average) (μ inches)			Equivalent Static Load (lb)		Dynamic Load (lb)	Analytical Stresses Neglecting Inertia of Masses (lb/in^2)		Analytical Stresses Considering Inertia of Masses (lb/in^2)		Experimental Stresses (lb/in^2)	
h	ε_A	ε_B	ε_C	P_N	P_C	P_D	σ_1	σ_3	σ_1	σ_3	σ_1	σ_3
0.5	46	108	91	59	38	199	7845	-193	5072	-125	3934	1816
1	69	204	103	81	52	332	10797	-265	6862	-169	6397	816
1.5	80	229	119	98	62	374	13065	-321	8239	-202	7244	1113
2	94	260	143	112	71	432	14978	-368	9402	-231	8340	1627

P_N = Inertia of Masses Neglected $\qquad$ P_C = Inertia of Masses Considered

From Dally and Riley[8]

$$\sigma_1 = E\left[\frac{\varepsilon_A + \varepsilon_C}{2(1-\gamma)} + \frac{1}{2(1+\gamma)}\left((\varepsilon_A - \varepsilon_C)^2 + (2\varepsilon_B - \varepsilon_A - \varepsilon_C)^2\right)^{\frac{1}{2}}\right]$$

$$\sigma_3 = E\left[\frac{\varepsilon_A + \varepsilon_C}{2(1-\gamma)} - \frac{1}{2(1+\gamma)}\left((\varepsilon_A - \varepsilon_C)^2 + (2\varepsilon_B - \varepsilon_A - \varepsilon_C)^2\right)^{\frac{1}{2}}\right]$$

---

[8] J. W. Dally and W. F. Riley, Experimental Stress Analysis (McGraw-Hill Book Company, 1965) p. 427.

TABLE 2

RESULTS OF STATIC TESTS

ε_A	ε_B	ε_C	σ_1	σ_3
15	125	55	3620.95	-683.89
21	196	95	5769.15	-902.01
30	265	130	7830.67	-1117.39
35	325	170	9729.03	-1127.63

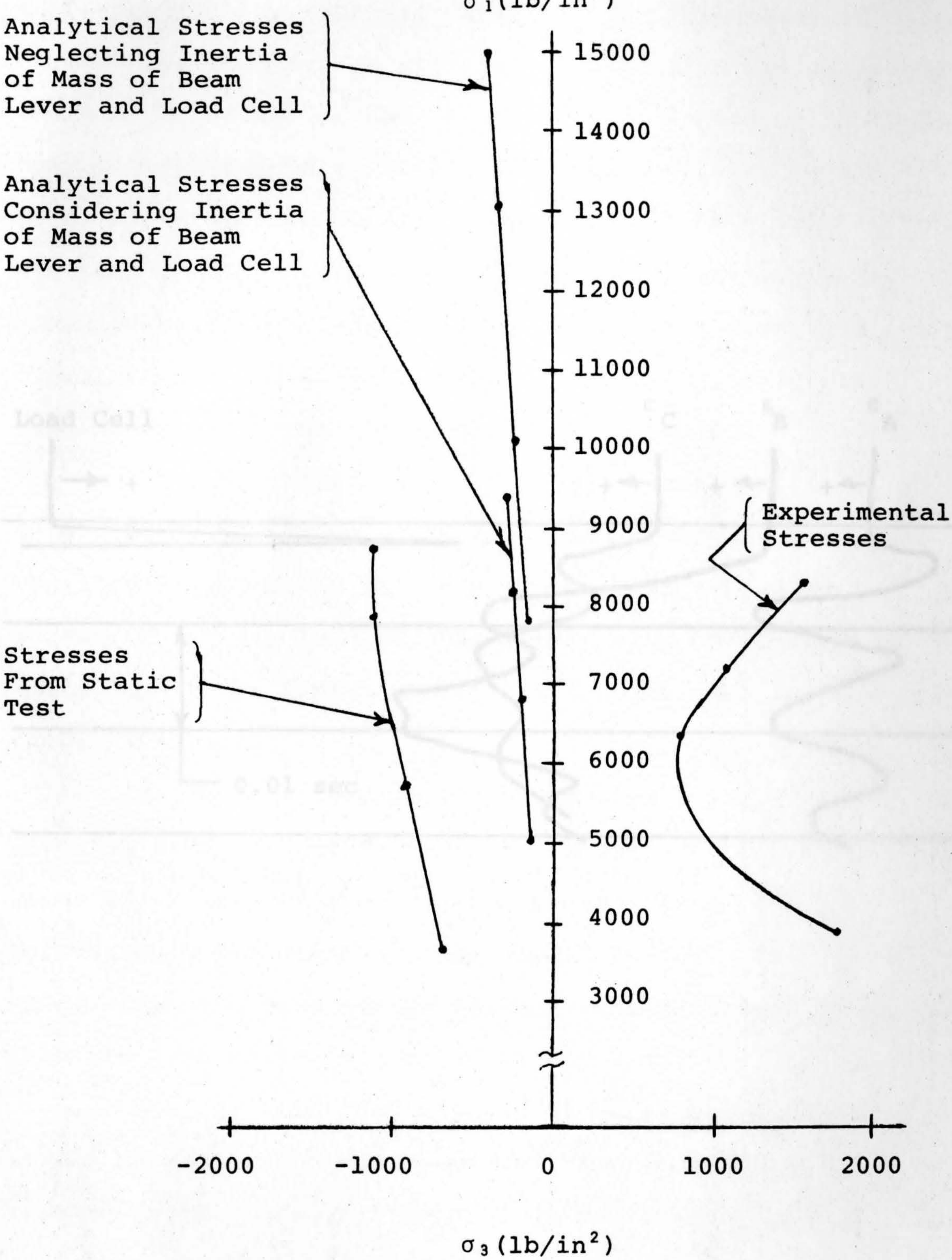

Fig. 9. Graph of Principal Stresses Obtained by Analytical and Experimental Means.

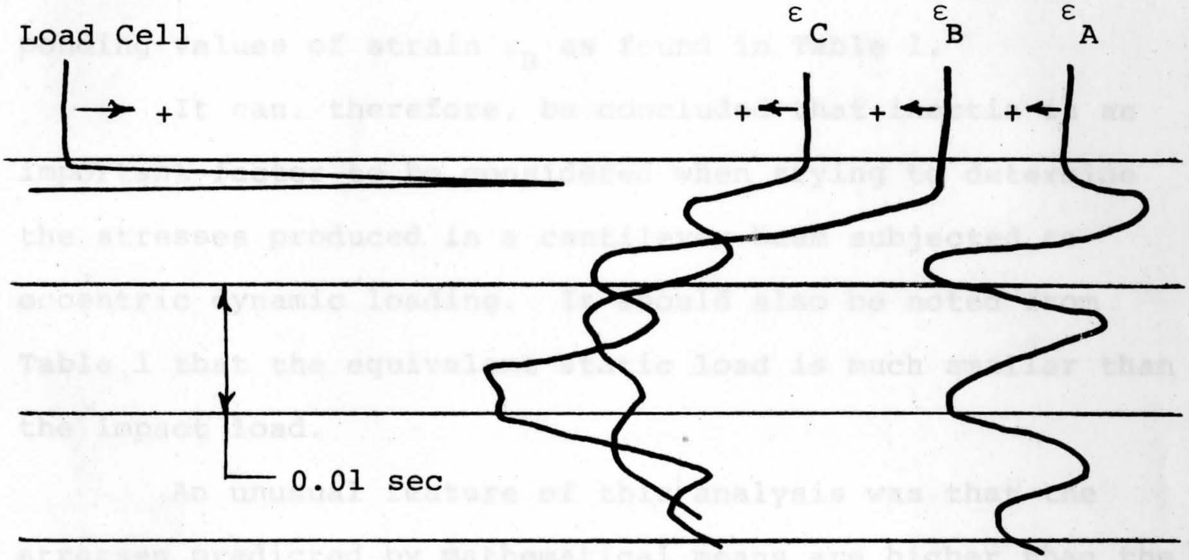

Fig. 10. Example of Experimental Strains Recorded on Strip Chart for ½ Inch Drop Height of Weight.

corresponding experimental value of σ_3. This trend of σ_3 to become less negative as inertia is considered indicates that the inertia effect of the relatively large mass of the load cell (2½ lb) tended to reduce the torque applied to the beam. This becomes readily apparent when the graph of the stresses for the static test is studied. For this case, where inertia obviously plays no part, it is seen that the σ_3 values have moved in a negative direction for corresponding values of strain ε_B as found in Table 1.

It can, therefore, be concluded that inertia is an important factor to be considered when trying to determine the stresses produced in a cantilever beam subjected to eccentric dynamic loading. It should also be noted from Table 1 that the equivalent static load is much smaller than the impact load.

An unusual feature of this analysis was that the stresses predicted by mathematical means are higher than the experimental stresses when yielding is assumed to occur according to the Maximum Shear Stress Theory. For the usual case, where the mass of the falling weight is much greater than the mass of the member it is striking, the stresses predicted by mathematical means will be much less than the actual stresses produced. However, for the case that was treated in this thesis, the mass of the falling weight was less than the combined masses of the beam, lever and load cell which apparently caused this reciprocal effect of the normal rule. In any event, the energy method, as applied here, showed considerable deviation in it's stress predictions from the actual experimental stress values and gives substance to the reason that the energy method is sometimes referred to as the approximate method. As far as mathematical simplicity, it has it's advantages, however, if more exact results are required, other techniques will have to be used which take into consideration such things as non-plastic impact, propagation of stress waves in the body, heat loss at impact and better modeling of the velocity of the elastic line of the beam and eccentric lever.

Another factor that should be considered is the effect of torsional inertia which results from the twisting of the beam through the angle ϕ by the applied torque. This effect was neglected for the analysis which considered the inertia of the components in order to provide a relatively direct solution. To include this effect presents considerable mathematical difficulty, however, it's inclusion should shift the plot of the analytical values of stress, in Fig. 9, closer to the experimental values.

BIBLIOGRAPHY

Books

Cernica, John N. Strength of Materials. New York: Holt, Rinehart and Winston, Inc., 1966.

Dally, J. W. and Riley, W. F. Experimental Stress Analysis. New York: McGraw-Hill Book Company, 1965.

D'Isa, Frank A. Mechanics of Metals. Reading, Mass.: Addison-Wesley Publishing Company, 1968.

Spotts, M. F. Design of Machine Elements. Englewood Cliffs, N. J.: Prentice-Hall, Inc., 1971.

Streidel, Robert F. Jr. An Introduction to Mechanical Vibrations. New York: John Wiley & Sons, Inc., 1971.